RSC Advances

PAPER

View Article Online
View Journal | View Issue

Cite this: *RSC Adv.*, 2023, **13**, 35985

The preparation and characterization of self-healing hydrogels based on polypeptides with a dual response to light and hydrogen peroxide†

Congwei Wang,[a] Dinglei Zhao,[b] Yongjun Xie,*[b] Qiang Zhou[b] and Haiyang Yang *[b]

Injectable self-healing hydrogels are being widely used in drug delivery, tissue engineering, and other fields. Because of their excellent biocompatibility and biodegradability, polypeptides are an ideal candidate for preparing injectable self-healing hydrogels. In this study, a polypeptide-based hydrogel with dual response to hydrogen peroxide and light was obtained by copolymerizing 4-arm PEG-amine, *N*-(*p*-nitrophenoxycarbonyl)-L-methionine, and *N*-(*p*-nitrophenoxycarbonyl)-γ-*o*-nitrobenzyl-L-glutamate. The hydrogel exhibits injectable self-healing behavior due to the hydrophobic interactions among peptide blocks, which also act as the reservoir of hydrophobic drug molecules. In the presence of hydrogen peroxide or under light irradiation, the thioether bond in methionine was oxidized to sulfoxide, whereas the *o*-nitro benzyl ester bond was broken to form glutamic acid. As a result, the corresponding hydrophobic blocks of polypeptide become hydrophilic, accelerating the release of drug molecules loaded in the polypeptide hydrophobic blocks. Using this technique, the controlled release of hydrophobic drug molecules was achieved. Our efforts could provide a new strategy for the preparation of self-healing hydrogels based on polypeptides with a dual response to hydrogen peroxide and light. In this view, the practical application of polypeptides in drug delivery, tissue engineering, and other fields, could be expanded and advanced.

Received 30th July 2023
Accepted 23rd November 2023

DOI: 10.1039/d3ra05156k

rsc.li/rsc-advances

Introduction

In recent years, stimulation-responsive and self-healing hydrogels have attracted extensive attention because of their great potential applications in a number of fields, such as drug delivery and tissue engineering.[1–3] Among various types of hydrogels, the injectable self-healing hydrogels, which can enter the human body through a syringe injection, thus avoiding the injury caused by surgical incisions in patients, have attracted special attention in the field of drug delivery.[4–7] Owing to their interactions, such as hydrogen bonding,[8] π–π stacking,[9] electrostatic interaction,[10] and hydrophobic interaction,[11–13] polypeptides can easily self-assemble into supramolecular structures. In particular, polypeptides have excellent biocompatibility and biodegradability. Therefore polypeptides are the ideal candidates for preparing injectable self-healing hydrogels for drug delivery and tissue engineering. The effective incorporation of drug molecules into polypeptides and their effective release at target locations is an area that needs further investigation.

Stimulation-responsive hydrogels can change their physical and chemical properties under stimulation to achieve targeted and controlled drug release.[14] So far, commonly used stimuli include temperature,[15,16] light,[12,17] pH,[18] enzymes,[19] and ROS,[20] which are also one of the commonly used internal stimuli in targeted anticancer drug delivery.[21] According to literature reports, high concentrations of reactive oxygen species have been found in most types of tumor tissues. Hydrogen peroxide, a reactive oxygen species having the highest concentration and best stability, is mainly produced in cell membranes, mitochondria, endoplasmic reticulum, and phagosomes and can freely diffuse among cells.[22–25] The pendent group - thioether bond in L-methionine is a reactive oxygen species-responsive group. Numerous studies have reported that L-methionine in proteins can be easily oxidized by reactive oxygen species to sulfoxides or sulfones.[26,27] L-Methionine exhibits a transition between hydrophobicity and hydrophilicity while responding to the reactive oxygen species.[20] In our previous study,[28] we found that if the reactive methionine monomer is polymerized *in situ* in the presence of water using 4-arm PEG-amine as an initiator, the hydrogels based on polypeptide can be conveniently obtained. In the presence of hydrogen peroxide, the thioether bond in methionine is oxidized to sulfoxide. As a result, the corresponding hydrophobic blocks of the polypeptide

[a]*Key Laboratory of Biomimetic Sensor and Detecting Technology of Anhui Province, School of Materials and Chemical Engineering, West Anhui University, Lu'an, 237012, Anhui Province, P. R. China*

[b]*CAS Key Laboratory of Soft Matter Chemistry, School of Chemistry and Materials Science, University of Science and Technology of China, Hefei, 230026, P. R. China. E-mail: yhy@ustc.edu.cn*

† Electronic supplementary information (ESI) available. See DOI: https://doi.org/10.1039/d3ra05156k

become hydrophilic. As a result, the hydrogels undergo the sol–gel transition owing to the action of hydrogen peroxide. Using doxorubicin as a model molecule for drug release simulation experiments, we have found that the release of doxorubicin loaded in the hydrogels was significantly accelerated, mainly because the corresponding hydrophobic blocks of polypeptide became hydrophilic in the presence of hydrogen peroxide.

However, if the polypeptide-based hydrogels were obtained by copolymerizing 4-arm PEG-amine with *N*-(*p*-nitrophenoxycarbonyl)-L-methionine alone, the encapsulated drugs should be easy to leak into humans under physicochemical conditions because the hydrophobic interactions among peptide blocks, which also act as reservoirs of hydrophobic drug molecules, are not strong enough. It is already known that light stimulus is a remote external stimulus source that can easily and conveniently modulate the mechanical properties of hydrogels in time and space.[29–37] Deming *et al.* reported that hydrogels based on polylysine modified with photoresponsive groups were used for controlled load release. When the hydrogels were exposed to UV light, they degraded to release the dye molecules loaded therein.[38] Yin *et al.* reported that photoresponsive polyglutamic acid can also be used for DNA delivery.[39]

In order to control the physicochemical properties of the hydrogels more effectively[40–42] and modulate the release of the loaded drug more precisely, the new hydrogels based on a polypeptide, with dual response to hydrogen peroxide and light, by copolymerizing 4-arm PEG-amine, methionine *N*-carboxylic anhydride, and *o*-nitro benzyl glutamate *N*-carboxylic anhydride, is reported here. The hydrophobic interaction among the polypeptide blocks not only endows the hydrogels with self-healing properties but also provides hydrophobic micro-regions for loading hydrophobic drugs. In the presence of hydrogen peroxide or under light irradiation, the thioether bond in methionine was oxidized to sulfoxide whereas the *o*-nitro benzyl ester bond was broken to form glutamic acid. As a result, the corresponding hydrophobic blocks of the polypeptide became hydrophilic, accelerating the release of the drug molecules loaded among the polypeptide hydrophobic blocks. According to this technique, the controlled release of the hydrophobic drug molecules at specific sites such as tumor tissues in a physiological environment was realized.

Experimental

Materials and methods

p-Nitrophenyl chloroformate was purchased from Meyer Chemical Co. Ltd. without further purity. L-Glutamate acid (Aladdin) was used as received. 1,1,3,3-Tetramethylguanidine (TMG, 98%, Aldrich) was distilled under reduced pressure. Tetra-PEG-NH_2 was purchased from Sigma-Aldrich. DOX·HCl was obtained from J and K Chemicals. *N*,*N*-Dimethylacetamide (extra dry, with molecular sieves, water ≤ 50 ppm), and *o*-nitrobenzyl alcohol were purchased from Energy Chemicals. All other reagents were purchased from Sinopharm Chemical Reagent Co Ltd. and used as received. Water was deionized using a Milli-Q SPreagent water system (Millipore) to a specific resistivity of 18.4 mΩ cm.

^{1}H NMR (300 MHz) spectra were acquired using a 300 MHz Bruker instrument. Molecular weight and molecular weight distributions, PDI, were determined by gel permeation chromatography (GPC) equipped with a Waters 1515 pump and a Waters 2414 differential refractive index detector (set at 30 °C). It used a series of three linear Styragel columns at an oven temperature of 45 °C. The eluent was DMF at a flow rate of 1.0 mL min^{-1}. A series of low polydispersity polystyrene standards were employed for calibration. The degrees of polymerization, DPs, were determined by ^{1}H NMR analysis. The rheological properties of the prepared hydrogels were studied using a rheometer (TA instruments, AR-G2) with a platform of 40 mm diameter.

Synthetic procedure

Synthesis of *N*-(*p*-nitrophenoxycarbonyl)-γ-*o*-nitrobenzyl-L-glutamate. The brief synthesis process is as follows: first, *o*-nitrobenzene methane was brominated with phosphorus tribromide to produce *o*-nitrobenzyl bromide, which was directly used for the next reaction without purification. Subsequently, under the catalysis of *N*,*N*,*N*′,*N*′-tetramethyl guanidine, *o*-nitro benzyl bromide was added to a copper-protected glutamic acid solution and reacted for 38 hours to obtain copper-protected *o*-nitro benzyl glutamate, and then, copper ions were removed under the action of ethylene diamine tetraacetic acid to obtain white *o*-nitro benzyl glutamate, which was further purified through recrystallization (Scheme 1).

p-Nitrophenyl chloroformate was added dropwise to the solution of *o*-nitro benzyl glutamate, and the temperature was raised to 40 °C while stirring overnight. After the reaction was completed, the obtained product was separated by column chromatography to obtain a white solid.

Synthesis of monomer *N*-(*p*-nitrophenoxycarbonyl)-L-methionine. The brief synthesis process is as follows: *p*-nitrophenyl chloroformate was added dropwise to a L-methionine solution at room temperature; then, the thus obtained mixture was warmed to 40 °C and stirred overnight. After the reaction was completed, the obtained product was separated with column chromatography to obtain a white solid.

Hydrogel preparation. The hydrogel was prepared by dispersing star polypeptide-PEG conjugates in water. The obtained solutions were gently heated and vigorously stirred for a few minutes to ensure complete dissolution. The solutions were then cooled to room temperature to allow gelation.

Rheological measurements of the hydrogels. The rheological properties of all the prepared hydrogels were studied using a rheometer (TA AR-G2) with a platform of 40 mm diameter. The frequency-sweep measurement was conducted in a constant-strain (0.5%) mode over the frequency range of 0.1–100 rad s^{-1} at 37 °C. Before studying the self-healing property, a strain-sweep measurement was conducted at a constant frequency of 6.283 rad s^{-1} over the strain range of 0.1% to 100% at 37 °C. Finally, a strain step cycled between 1% and 70% was performed at 37 °C and 6.283 rad s^{-1}.

Preparation of DOX-loaded hydrogel and controlled release of the DOX payload. Typically, 30 mg DOX·HCl was dissolved in

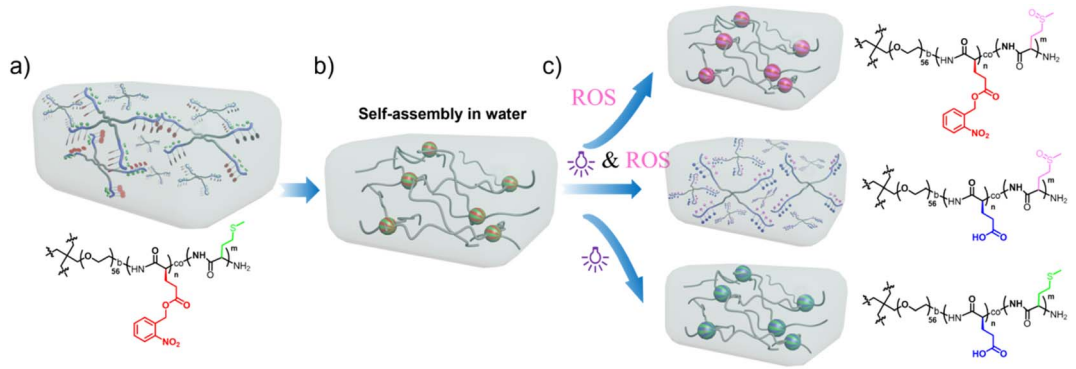

Scheme 1 A schematic illustration of the design of the hydrogels with dual response to light and hydrogen peroxide. (a) Th structure of polypeptides. (b) Polypeptides dissolve in water and assemble to form the hydrogel owing to the hydrophobic interactions. (c) The degradation mechanism of hydrogels stimulated by light, ROS (reactive oxygen species), and both light and ROS.

1 mL DMSO and 2 mL of triethylamine was added and stirred at room temperature, overnight. After that, 300 mg of the polymer was added and stirred at ambient temperature for 2 h. The mixtures were then subjected to dialysis against PBS buffer (pH 7.4, 10 mM) for 24 h to remove unloaded DOX and the DMSO solvent. The dialysate was adjusted to predetermined volumes (pH 7.4, 10 mM) by adding PBS buffer. According to a standard calibration curve, the DOX loading efficiencies (LE) and the DOX loading contents (LC) were estimated. For the triggered release of DOX, in a typical release experiment, DOX-loaded hydrogels (500 μL) were transferred to a dialysis cell with a molecular weight membrane (MWCO: 3.5 kDa) and then dialyzed against 9.5 mL of PBS buffer (pH 7.4, 10 mM) at 37 °C. The released DOX concentrations in the dialysate were quantified by measuring the absorption intensities at 480 nm for DOX against the corresponding standard calibration curves.

***In vitro* cytotoxicity measurement.** Cell viability was examined by the MTT assay. HeLa cells were seeded in a 96-well plate at a density of 10^4 cells per well in 100 μL of the DMEM medium with 10% FBS at 37 °C under a 5% CO_2 humidified atmosphere. Drug-loaded micelles with or without 30 min of UV irradiation (1 mW cm^{-2}) were then added to target a final concentration of 3.0 g L^{-1}. After incubating for 24 h, the MTT reagent (in 20 μL of the PBS buffer, 5 mg mL^{-1}) was added to each well, and the cells were further incubated with 5% CO_2 for 4 h at 37 °C. The culture medium in each well was removed and replaced by 150 μL of DMSO. The solution from each well was transferred to another 96-well plate, and the absorbance values were recorded at a wavelength of 490 nm using a microplate reader (Thermo Fisher). Cell viability was calculated using the equation, $A_{490,\text{treated}}/A_{490,\text{control}} \times 100\%$, where $A_{490,\text{treated}}$ and $A_{490,\text{control}}$ are the absorbance values in the presence and absence of the polymeric micelles, respectively. Each experiment was performed in quadruple, and the data are shown as the mean value.

Results and discussion

Preparation process of the organogel/hydrogel hybrids

Synthesis and characterization of star polypeptide-PEG conjugates. A typical polymerization process is shown in Scheme 2. Monomers *N*-(*p*-nitrophenoxycarbonyl)-L-methionine and *N*-(*p*-nitrophenoxycarbonyl)-γ-*o*-nitrobenzyl-L-glutamate were dissolved in toluene, and the initiator *tetra*-PEO_{56}-NH_2 was added; the trace water contained in the solvent was removed through azeotropy, and dry *N*,*N*-dimethyl acetamide solvent was injected using a syringe under vacuum conditions, and the obtained mixture was sealed in a reaction tube and heated to 60 °C for polymerization for 48 hours. After the polymerization, the obtained solution was poured into an excess ether solvent and precipitated three times to obtain a white powder, which was then dried at room temperature in a vacuum-drying oven.

The monomer conversion and mean degree of polymerization (DP) were determined using ^{1}H NMR from the ratio of the characteristic peak of the benzyl group on *o*-nitrobenzyl-L-glutamate at 5.5 ppm and the characteristic peak of the methylene group on the side chain of L-methionine at 2.55 ppm, and the characteristics of the PEG moiety at 3.5 ppm. The number-average molecular weight (M_n) was determined by ^{1}H NMR analysis, and polydispersity index (PDI, M_w/M_n) was quantified using gel permeation chromatography (Fig. 1).

Rheological characterization of hydrogels. To quantify the mechanical properties of the star polypeptide-PEG conjugates, a series of hydrogels with different compositions and concentrations were prepared. The frequency sweep measurements of different compositions and concentrations of hydrogels were performed (Fig. 2).

The mechanical properties of the hydrogel also appeared to be relevant to the normal development, differentiation, and motility of cell. We finally chose *t*-PEG_{56}-*b*-P ($NBLG_5$-*co*-$Meth_7$) hydrogel with 40 wt% solid content for the next experiments,

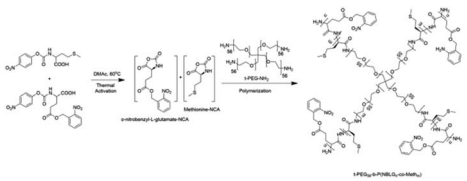

Scheme 2 The synthetic route of star polypeptide-PEG conjugates.

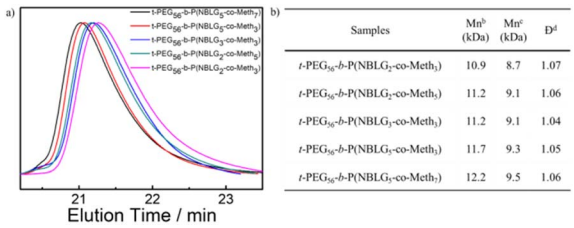

Samples	Mn^b (kDa)	Mn^c (kDa)	$Đ^d$
t-PEG$_{56}$-*b*-P(NBLG$_2$-*co*-Meth$_3$)	10.9	8.7	1.07
t-PEG$_{56}$-*b*-P(NBLG$_2$-*co*-Meth$_5$)	11.2	9.1	1.06
t-PEG$_{56}$-*b*-P(NBLG$_3$-*co*-Meth$_3$)	11.2	9.1	1.04
t-PEG$_{56}$-*b*-P(NBLG$_5$-*co*-Meth$_3$)	11.7	9.3	1.05
t-PEG$_{56}$-*b*-P(NBLG$_5$-*co*-Meth$_7$)	12.2	9.5	1.06

Fig. 1 (a) The GPC analysis of star polypeptide-PEG conjugates using DMF as the eluent. (b) The summary table of the conjugate structure parameters.

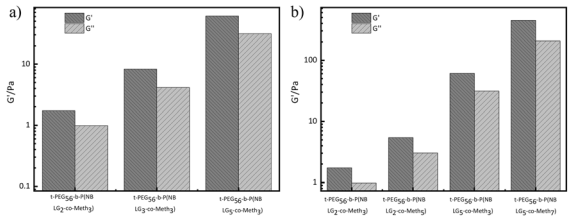

Fig. 3 The storage modulus and loss modulus of conjugates with different polymerization degree at a 40% solid content (a) *t*-PEG$_{56}$-*b*-P (NBLG$_2$-*co*-Meth$_3$), *t*-PEG$_{56}$-*b*-P (NBLG$_3$-*co*-Meth$_3$), and *t*-PEG$_{56}$-*b*-P (NBLG$_5$-*co*-Meth$_3$). (b) *t*-PEG$_{56}$-*b*-P (NBLG$_2$-*co*-Meth$_3$), *t*-PEG$_{56}$-*b*-P (NBLG$_2$-*co*-Meth$_5$), *t*-PEG$_{56}$-*b*-P (NBLG$_5$-*co*-Meth$_3$) and *t*-PEG$_{56}$-*b*-P (NBLG$_5$-*co*-Meth$_7$).

because it has the mechanical strength matching to that of the normal human soft tissue (Fig. 3).

Self-healing and injectability of the hydrogel. Hydrogels with self-healing ability would enable them to self-repair when damaged by external pressure, thus extending the serviceable range and lifespan. Before the self-repair test, a shear thinning test was carried out on the hydrogels to determine the linear viscoelastic zone and the strain point for the gel–sol transition of the hydrogels.

Fig. 4a shows the changes in the storage modulus and loss modulus of *t*-PEG$_{56}$-*b*-P (NBLG$_5$-*co*-Meth$_7$) hydrogels with 40 wt% solid content under strain scanning. Under small strain, the storage modulus and loss modulus of the hydrogels remained unchanged and the storage modulus was greater than the loss modulus (strain $\gamma < 10\%$). Under the increased strain, the storage modulus and loss modulus of the hydrogels began to decline, and the storage modulus decreased faster than the loss modulus, finally, the storage modulus and loss modulus of the hydrogel intersected under the ground strain $\gamma = 70\%$, and then the loss modulus became greater than the storage modulus, which indicated that the hydrogels were converted by the sol transition, and the cross-linking network inside the hydrogels was destroyed. This excellent shear-thinning property of the prepared hydrogel makes it possible for injection with a syringe.

The self-healing properties of the hydrogels can be verified by dynamic strain scanning under a strain of 0.1% or 70% (Fig. 4b). At the initial stage, 0.1% strain was applied to the hydrogels. The storage modulus of the hydrogels was approximately 0.37 kPa and the loss modulus was 0.28 kPa. Under this strain, the storage modulus was greater than the loss modulus and substantially remained unchanged. When the strain applied to the hydrogels was changed to 70%, the storage modulus of the hydrogels immediately dropped from about 0.37 kPa to about 0.18 kPa, but the loss modulus only dropped from 0.28 kPa to 0.22 kPa. Under this strain, the storage modulus was less than the loss modulus and remained substantially unchanged. Then, the strain applied to the hydrogels was recovered from 70% to 0.1%, and the storage modulus and loss modulus can be immediately restored to their initial state under small strain. The cyclic strain test results showed that the hydrogels have excellent self-healing properties, and their mechanical properties can be restored to the initial state after several different strain scans.

Photograph and rheological studies of the gel-to-sol transition upon application of stimuli. The responsiveness of the newly prepared hydrogel was investigated by tilting the vials. Before the stimulus was applied, the hydrogels in the tilted vial

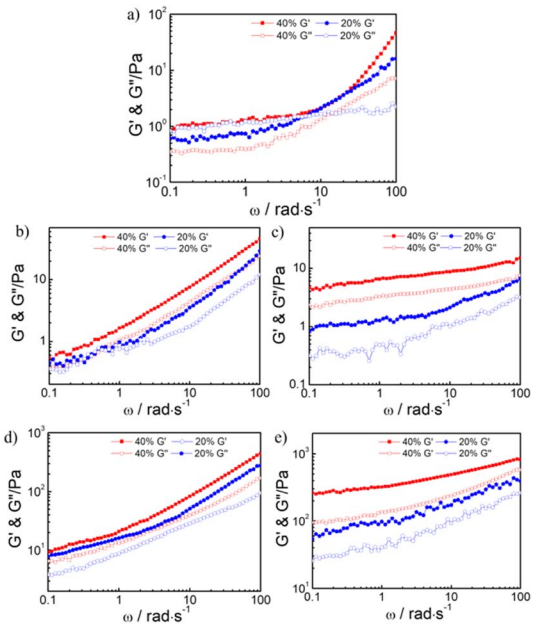

Fig. 2 The frequency-sweep measurements of hydrogel storage modulus, *G*′/Pa, and loss modulus, *G*″/Pa), for hydrogels of different compositions (a) *t*-PEG$_{56}$-*b*-P (NBLG$_2$-*co*-Meth$_3$), (b) *t*-PEG$_{56}$-*b*-P (NBLG$_2$-*co*-Meth$_5$), (c) *t*-PEG$_{56}$-*b*-P (NBLG$_3$-*co*-Meth$_3$), (d) *t*-PEG$_{56}$-*b*-P (NBLG$_5$-*co*-Meth$_3$), (e) *t*-PEG$_{56}$-*b*-P (NBLG$_5$-*co*-Meth$_7$) and concentrations (20 wt%, 40 wt%).

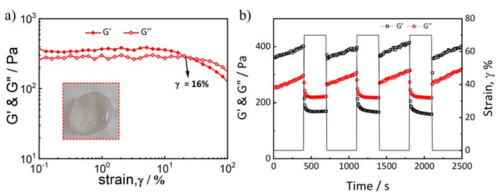

Fig. 4 (a) The strain-sweep measurements of a 40 wt% *t*-PEG$_{56}$-*b*-P (NBLG$_5$-*co*-Meth$_7$) hydrogel at 37 °C (the inset shows the state of the hydrogel at room temperature). (b) Repeated dynamic strain step tests ($\gamma = 0.1\%$ or 70%).

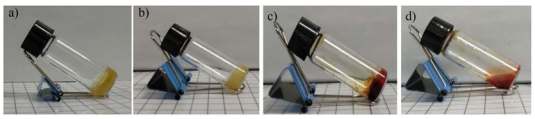

Fig. 5 (a–d) The photographs of the reversed vial test of the dual response process of hydrogels at 37 °C.

could not flow (Fig. 5a), which indicated that the hydrogels were in the gel state. When 10 μL of hydrogen peroxide was added to the vial, the color of the hydrogels gradually faded (Fig. 5b), but the hydrogels still could not flow in a tilted state. On the other hand, light irradiation was applied to the hydrogel for 30 minutes, and the color of the hydrogels gradually changed from light color to purple-red under the effect of the UV light (Fig. 5c), but the hydrogel still could not flow after tilting the vial. This showed that the gel sol transition of the hydrogels cannot occur with only one stimulus.

Finally, 10 μL of hydrogen peroxide was added to the vial and then the vial was irradiated with UV light for 30 minutes. In the process of radiation, the hydrogels gradually turned red, at the same time the tilted hydrogels in the vial gradually recovered to an equilibrium state (Fig. 5d). The sample was found to flow by shaking the vial, indicating that the hydrogels had undergone a complete gel–sol transition and degraded to a solution.

Furthermore, frequency-sweep measurements of hydrogels in different states were performed. As shown in Fig. 6a–d, the storage moduli (G') was larger than the loss moduli (G''), indicating the sample was in the gel state. After double stimuli, the storage moduli (G') was smaller than the loss moduli (G''), indicating the gel degraded to a fluidic solution (Fig. 6d). The hydrogels without any stimulation showed a significant shear thinning behavior, which indicated that the hydrogels were injectable. The gel weakened significantly after stimulation by UV radiation or hydrogen peroxide, and the viscosity of the gel decreased significantly when stimulated by both UV radiation and hydrogen peroxide (Fig. S3†).

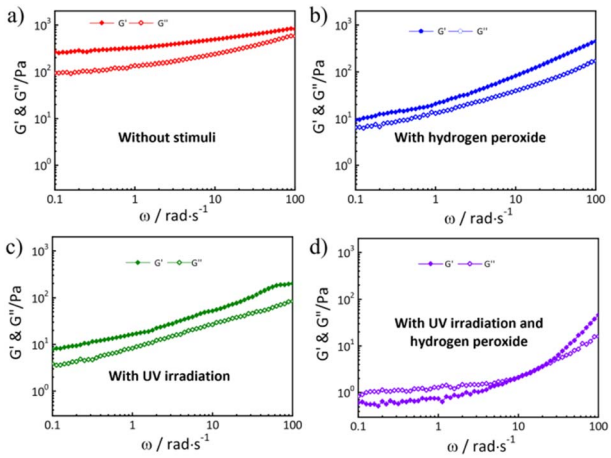

Fig. 6 The frequency-sweep measurement of the hydrogel (*t*-PEG56-*b*-P (NBLG5-*co*-Meth$_7$) was performed at different stimuli at 37 °C: (a) without stimuli, (b) with hydrogen peroxide, (c) with UV irradiation, and (d) with UV irradiation and hydrogen peroxide.

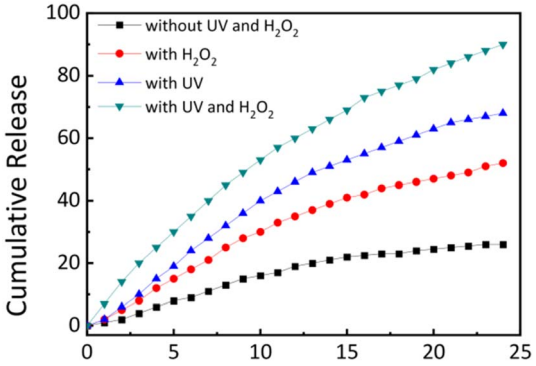

Fig. 7 A cumulative DOX release profile from the drug-loaded hydrogel (pH 7.4 buffer, 37 °C) with different stimuli.

Stimuli-regulated release profile of doxorubicin. Doxorubicin was used as a model drug for the cumulative release of the drug-loaded hydrogels. According to the cumulative release of doxorubicin, we calculated that the effective load of doxorubicin in the hydrogels was 4%, and the load efficiency was 40%. Release kinetics of the loaded drug were obtained by placing the hydrogels loaded with doxorubicin in a dialysis bag and measuring the UV absorbable value at 480 nm in dialysate compared with the absorption curve of the standard concentration (Fig. S4†).

The results are shown in Fig. 7. The cumulative release curve of the hydrogels without any external stimulus was first investigated. Under the condition of 37 °C and pH 7.4, the cumulative release of doxorubicin loaded in the hydrogels was only 26% within 24 hours. In the presence of hydrogen peroxide, the release rate of the loaded doxorubicin increased and ultimately reached 52% after 24 hours.

In contrast, light irradiation stimulus has a stronger accelerating effect on the release of doxorubicin, ultimately accumulating 68% of doxorubicin after 24 hours. This may be due to the generation of the carboxyl negative ions after the bond breakage caused by light, which accelerates the release of doxorubicin by the reduction of hydrophobic interactions and repulsiveness among negative charges. Finally, under the combined action of hydrogen peroxide and ultraviolet light, the release rate of doxorubicin was significantly increased, and 90% of doxorubicin was ultimately released within 24 hours. Hydrogen peroxide combined with light accelerated the release of doxorubicin loaded in the hydrogels in the target site.

Cytotoxicity of the drug-loaded conjugates. We examined the cytotoxicity of *t*-PEG$_{56}$-*b*-P (NBLG$_5$-*co*-Meth$_7$) micelles *in vitro* cells using the MTT assay against HeLa cells (Fig. 8). The cell viability of the drug-free blank micelles without stimuli remained to be ~94% at 3.0 g L^{-1} polymer concentration, suggesting that the conjugate micelles were almost non-cytotoxic. When HeLa cells were incubated with DOX-loaded micelles without stimuli, ~72% of cells survived at 3.0 g L^{-1} polymer concentration. The cell viability decreased further when the DOX-loaded micelles with 10 μL hydrogen peroxide were added to the cell culture medium and only 58% of the cells survived. When DOX-loaded micelles, after 30 min of UV irradiation, were added to the cell culture medium, the cell viability

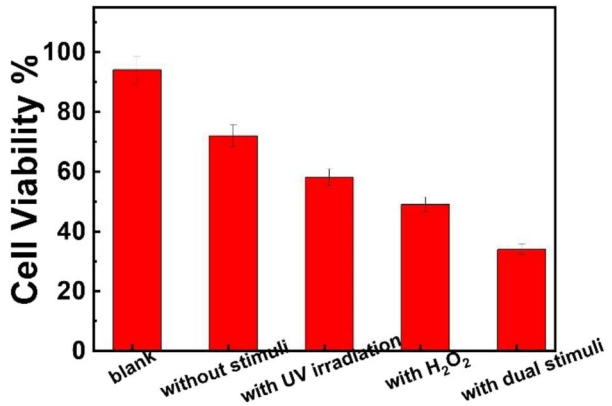

Fig. 8 A comparison of MTT cytotoxicity assay results of *t*-PEG56-*b*-P(NBLG5-*co*-$Meth_7$) micelles under different stimuli.

decreased further and only 49% of the cells survived. When the DOX-loaded micelles after dual stimuli were added to the cell culture medium, the final cell viability decreased only to 34%. The statistically significant difference was confirmed by the Student's test with $p < 0.05$. This result is also in agreement with the discrepancy in drug release profiles for different stimuli.

Conclusions

Herein, an injectable self-healing hydrogel, based on polypeptides and responsive to hydrogen peroxide and light, was prepared. Due to the hydrophobic interactions among peptide blocks, which also act as the reservoir of hydrophobic drug molecules, the hydrogel exhibits injectable self-healing behavior. In the presence of hydrogen peroxide or under light irradiation, the thioether bond in methionine was oxidized to sulfoxide, whereas the *o*-nitro benzyl ester bond was broken to form glutamic acid. As a result, the corresponding hydrophobic blocks of the polypeptide became hydrophilic, accelerating the release of the drug molecules loaded among the polypeptide hydrophobic blocks. The controlled release of the hydrophobic drug molecules at specific sites such as tumor tissues was realized accordingly.

Conflicts of interest

There are no conflicts to declare.

Acknowledgements

This work was supported by the National Science Foundation of China (Grant no 51273189), the National Science and Technology Major Project of the Ministry of Science and Technology of China (2016ZX05016), and the National Science and Technology of China (2016ZX05046).

Notes and references

1 M. R. Islam, Y. Gao, X. Li, *et al.*, Responsive polymers for biosensing and protein delivery, *J. Mater. Chem. B*, 2014, **2**(17), 2444–2451.
2 J. L. Drury and D. J. Mooney, Hydrogels for tissue engineering: scaffold design variables and applications, *Biomaterials*, 2003, **24**(24), 4337–4351.
3 M. E. Roth-Konforti, M. Comune, M. Halperin-Sternfeld, *et al.*, UV Light-Responsive Peptide-Based Supramolecular Hydrogel for Controlled Drug Delivery, *Macromol. Rapid Commun.*, 2018, **39**(24), 1800588.
4 L. Yu and J. Ding, Injectable hydrogels as unique biomedical materials, *Chem. Soc. Rev.*, 2008, **37**(8), 1473–1481.
5 H. Tan and K. G. Marra, Injectable, Biodegradable Hydrogels for Tissue Engineering Applications, *Materials*, 2010, **3**(3), 1746–1767.
6 M. K. Nguyen and D. S. Lee, Injectable Biodegradable Hydrogels, *Macromol. Biosci.*, 2010, **10**(6), 563–579.
7 C. He, S. W. Kim and D. S. Lee, In situ gelling stimuli-sensitive block copolymer hydrogels for drug delivery, *J. Controlled Release*, 2008, **127**(3), 189–207.
8 D. J. Adams and P. D. Topham, Peptide conjugate hydrogelators, *Soft Matter*, 2010, **6**(16), 3707–3721.
9 Y. Kuang and B. Xu, Disruption of the Dynamics of Microtubules and Selective Inhibition of Glioblastoma Cells by Nanofibers of Small Hydrophobic Molecules, *Angew. Chem., Int. Ed.*, 2013, **52**(27), 6944–6948.
10 A. Aggeli, M. Bell, N. Boden, *et al.*, Responsive gels formed by the spontaneous self-assembly of peptides into polymeric β-sheet tapes, *Nature*, 1997, **386**(6622), 259–262.
11 C. Chen, D. Wu, W. Fu, *et al.*, Peptide Hydrogels Assembled from Nonionic Alkyl-polypeptide Amphiphiles Prepared by Ring-Opening Polymerization, *Biomacromolecules*, 2013, **14**(8), 2494–2498.
12 D. Zhao, Q. Tang, Q. Zhou, *et al.*, A photo-degradable injectable self-healing hydrogel based on star poly(ethylene glycol)-b-polypeptide as a potential pharmaceuticals delivery carrier, *Soft Matter*, 2018, **14**(36), 7420–7428.
13 V. K. Kotharangannagari, A. Sánchez-Ferrer, J. Ruokolainen, *et al.*, Thermoreversible Gel–Sol Behavior of Rod–Coil–Rod Peptide-Based Triblock Copolymers, *Macromolecules*, 2012, **45**(4), 1982–1990.
14 L. Dong, A. K. Agarwal, D. J. Beebe, *et al.*, Adaptive liquid microlenses activated by stimuli-responsive hydrogels, *Nature*, 2006, **442**(7102), 551–554.
15 H. J. Oh, M. K. Joo, Y. S. Sohn, *et al.*, Secondary Structure Effect of Polypeptide on Reverse Thermal Gelation and Degradation of l/dl-Poly(alanine)–Poloxamer–l/dl-Poly(alanine) Copolymers, *Macromolecules*, 2008, **41**(21), 8204–8209.
16 H. J. Moon, D. Y. Ko, M. H. Park, *et al.*, Temperature-responsive compounds as in situ gelling biomedical materials, *Chem. Soc. Rev.*, 2012, **41**(14), 4860–4883.
17 M. He, J. Li, S. Tan, *et al.*, Photodegradable Supramolecular Hydrogels with Fluorescence Turn-On Reporter for Photomodulation of Cellular Microenvironments, *J. Am. Chem. Soc.*, 2013, **135**(50), 18718–18721.
18 Q. Tang, D. Zhao, H. Yang, *et al.*, A pH-responsive self-healing hydrogel based on multivalent coordination of Ni2+ with polyhistidine-terminated PEG and IDA-modified oligochitosan, *J. Mater. Chem. B*, 2019, **7**(1), 30–42.

19 J. Li, Y. Gao, Y. Kuang, *et al.*, Dephosphorylation of d-Peptide Derivatives to Form Biofunctional, Supramolecular Nanofibers/Hydrogels and Their Potential Applications for Intracellular Imaging and Intratumoral Chemotherapy, *J. Am. Chem. Soc.*, 2013, **135**(26), 9907–9914.

20 Q. Xu, C. He, K. Ren, *et al.*, Thermosensitive Polypeptide Hydrogels as a Platform for ROS-Triggered Cargo Release with Innate Cytoprotective Ability under Oxidative Stress, *Adv. Healthcare Mater.*, 2016, **5**(15), 1979–1990.

21 G. Saravanakumar, J. Kim and W. J. Kim, Reactive-Oxygen-Species-Responsive Drug Delivery Systems: Promises and Challenges, *Advanced Science*, 2017, **4**(1), 1600124.

22 Z. Deng, Y. Qian, Y. Yu, *et al.*, Engineering Intracellular Delivery Nanocarriers and Nanoreactors from Oxidation-Responsive Polymersomes via Synchronized Bilayer Cross-Linking and Permeabilizing Inside Live Cells, *J. Am. Chem. Soc.*, 2016, **138**(33), 10452–10466.

23 S. Yu, C. Wang, J. Yu, *et al.*, Injectable Bioresponsive Gel Depot for Enhanced Immune Checkpoint Blockade, *Adv. Mater.*, 2018, **30**(28), e1801527.

24 Q. Xu, C. He, C. Xiao, *et al.*, Reactive Oxygen Species (ROS) Responsive Polymers for Biomedical Applications, *Macromol. Biosci.*, 2016, **16**(5), 635–646.

25 C. Wang, J. Wang, X. Zhang, *et al.*, In situ formed reactive oxygen species–responsive scaffold with gemcitabine and checkpoint inhibitor for combination therapy, *Sci. Transl. Med.*, 2018, **10**(429), eaan3682.

26 S. Yamada, K. Koga, A. Sudo, *et al.*, Phosgene-free synthesis of polypeptides: Useful synthesis for hydrophobic polypeptides through polycondensation of activated urethane derivatives of α-amino acids, *J. Polym. Sci., Part A: Polym. Chem.*, 2013, **51**(17), 3726–3731.

27 J. Moskovitz, S. Bar-Noy, W. M. Williams, *et al.*, Methionine sulfoxide reductase (MsrA) is a regulator of antioxidant defense and lifespan in mammals, *Proc. Natl. Acad. Sci. U. S. A.*, 2001, **98**(23), 12920–12925.

28 D. Zhao, Q. Tang, Q. Zhou, *et al.*, A photo-degradable injectable self-healing hydrogel based on star poly (ethylene glycol)-b-polypeptide as a potential pharmaceuticals delivery carrier, *Soft Matter*, 2018, **14**(36), 7420–7428.

29 H. Yamamoto, T. Kitsuki, A. Nishida, *et al.*, Photoresponsive Peptide and Polypeptide Systems. 13. Photoinduced Cross-Linked Gel and Biodegradation Properties of Copoly(l-lysine) Containing ε-7-Coumaryloxyacetyl-l-lysine Residues, *Macromolecules*, 1999, **32**(4), 1055–1061.

30 S. Matsumoto, S. Yamaguchi, S. Ueno, *et al.*, Photo gel-sol/sol-gel transition and its patterning of a supramolecular hydrogel as stimuli-responsive biomaterials, *Chemistry*, 2008, **14**(13), 3977–3986.

31 A. M. Kloxin, A. M. Kasko, C. N. Salinas, *et al.*, Photodegradable Hydrogels for Dynamic Tuning of Physical and Chemical Properties, *Science*, 2009, (324), 59–63.

32 Y. Yang, J. Zhang, Z. Liu, *et al.*, Tissue-Integratable and Biocompatible Photogelation by the Imine Crosslinking Reaction, *Adv. Mater.*, 2016, **28**(14), 2724–2730.

33 G. Pasparakis, T. Manouras, P. Argitis, *et al.*, Photodegradable polymers for biotechnological applications, *Macromol. Rapid Commun.*, 2012, **33**(3), 183–198.

34 D. D. McKinnon, T. E. Brown, K. A. Kyburz, *et al.*, Design and characterization of a synthetically accessible, photodegradable hydrogel for user-directed formation of neural networks, *Biomacromolecules*, 2014, **15**(7), 2808–2816.

35 A. M. Kloxin, M. W. Tibbitt and K. S. Anseth, Synthesis of photodegradable hydrogels as dynamically tunable cell culture platforms, *Nat. Protoc.*, 2010, **5**(12), 1867–1887.

36 I. Tomatsu, K. Peng and A. Kros, Photoresponsive hydrogels for biomedical applications, *Adv. Drug Delivery Rev.*, 2011, **63**(14–15), 1257–1266.

37 M. A. Azagarsamy, D. D. McKinnon, D. L. Alge, *et al.*, Coumarin-Based Photodegradable Hydrogel: Design, Synthesis, Gelation, and Degradation Kinetics, *ACS Macro Lett.*, 2014, **3**(6), 515–519.

38 G. E. Negri and T. J. Deming, Triggered Copolypeptide Hydrogel Degradation Using Photolabile Lysine Protecting Groups, *ACS Macro Lett.*, 2016, **5**(11), 1253–1256.

39 L. Yin, H. Tang, K. H. Kim, *et al.*, Light-responsive helical polypeptides capable of reducing toxicity and unpacking DNA: toward nonviral gene delivery, *Angew. Chem., Int. Ed.*, 2013, **52**(35), 9182–9186.

40 M. K. Nguyen, C. T. Huynh, G. H. Gao, *et al.*, Biodegradable oligo(amidoamine/β-amino ester) hydrogels for controlled insulin delivery, *Soft Matter*, 2011, **7**(6), 2994–3001.

41 J. Zhuang, M. R. Gordon, J. Ventura, *et al.*, Multi-stimuli responsive macromolecules and their assemblies, *Chem. Soc. Rev.*, 2013, **42**(17), 7421–7435.

42 A. Fraix, R. Gref and S. Sortino, A multi-photoresponsive supramolecular hydrogel with dual-color fluorescence and dual-modal photodynamic action, *J. Mater. Chem. B*, 2014, **2**(22), 3443–3449.